

A Generic Sensor for Ultra Low Analyte Concentration Detection

J. Hedley*, C. J. McNeil*, J. S. Burdess*, A. J. Harris*, M. G. Dobson*, G. Suarez* and H. Berney*

*Institute for Nanoscale Science and Technology, Newcastle University,
Newcastle upon Tyne, NE1 7RU, England.

John.Hedley@ncl.ac.uk, Calum.McNeil@ncl.ac.uk, J.S.Burdess@ncl.ac.uk, Alun.J.Harris@ncl.ac.uk,
M.G.Dobson@newcastle.ac.uk, Guillaume.Suarez@newcastle.ac.uk, Helen.Berney@ncl.ac.uk

ABSTRACT

This paper reports on the development of a MEMS based generic mass sensor system (international patents pending) aimed at quantitative analyte measurement with a sensitivity of the order of 0.01 ng cm^{-2} . The sensor utilizes the property of cyclic symmetry to auto-compensate for any system drifts due to temperature fluctuations. Initial characterization of the sensor has demonstrated this auto-compensation mechanism. Immobilization protocols are currently being established using antibody immobilization onto a gold surface. The drive / sense electronics for the sensor system are under development.

Keywords: mass sensor, analyte detection, cyclic symmetry

1 INTRODUCTION

Measurement of mass using a resonant mechanical structure relies on added surface mass, produced by the immobilization of material onto the surface of the resonator, causing a shift in resonant frequency. Devices using this principle are referred to as micro-balances and are designed to use bulk, surface, or flexural acoustic waves to create resonant behaviour. Practical sensors have been manufactured using piezoelectric materials and well-known examples are the AT quartz shear wave resonator and the Rayleigh (SAW) resonator (see for example [1]-[4]). To achieve reliable measurements, particularly for low analyte concentrations, changes of the order of a few tens of hertz in a resonant frequency of 10~100 MHz must be detectable. Since these sensors rely on the unperturbed natural frequency of the resonator to provide an absolute reference it is important to have very stable operation or to account for parasitic frequency changes produced by temperature and the density and viscosity of any interfacial fluid. To overcome such problems adjacent matched resonator pairs can be used and the difference between their resonant frequencies taken as a measurement of added mass. This approach increases the cost and size of the basic system and there is the difficulty of producing two matched resonators.

In this project it was proposed to investigate the properties of cyclically symmetric structures and to explore how their special dynamic characteristics could be exploited to overcome the problems associated with the stability of the reference natural frequency. It is known that

the natural frequencies of such structures can form sets of degenerate pairs — i.e. two independent modes of vibration share a common natural frequency. The intention of this research was to choose a structure and make selected regions of the structure chemically active and modified with suitable species to provide sites for the specific binding of the desired analyte. Mass added to the structure at these specific sites will disrupt the symmetry of the structure and thus break the degeneracy. The natural frequencies of the two modes will then have unique values and their separation will determine the amount of added surface mass. By using MEMS technology and with this inherent calibration, this sensor is theoretically 100 times more sensitive than conventional single frequency sensors.

2 THEORY

The sensor is essentially a circular plate which is clamped at its edges. A solution to the vibration problem of a clamped plate has been given by Wah [5] and this will be briefly described here. The equation of motion for a plate is given by:

$$\nabla^4(w) - \frac{T}{D} \nabla^2(w) + \frac{\rho_s}{D} \frac{\partial^2 w}{\partial t^2} = 0, \quad (1)$$

where w is the deflection, ρ_s is the surface density and T is the tension (or compression) in the plate (force per unit length of edge). D is the flexural rigidity given by:

$$D = \frac{Eh^3}{12(1-\nu^2)} \quad (2)$$

where E is modulus of elasticity and ν is Poisson's ratio.

The general solution of (1), using cylindrical coordinates (r, θ) , is:

$$w = \left[A_n J_n \left(\frac{\alpha r}{a} \right) + B_n I_n \left(\frac{\beta r}{a} \right) \right] \times (\cos n\theta + \lambda_n \sin n\theta) \sin \omega t \quad (3)$$

where ω is the natural frequency of the plate, a is plate radius, n is the number of nodal diameters in the mode shape and:

$$\alpha^2 = \frac{Ta^2}{2D} \left[\left(1 + \frac{4\omega^2 \rho D}{T^2} \right)^{\frac{1}{2}} - 1 \right], \quad (4)$$

$$\beta^2 = \frac{Ta^2}{2D} \left[\left(1 + \frac{4\omega^2 \rho D}{T^2} \right)^{\frac{1}{2}} + 1 \right].$$

J_n , I_n are the Bessel and modified Bessel functions respectively. A_n , B_n and λ_n are arbitrary constants. For a clamped plate, the frequency equation becomes:

$$\alpha \frac{J_{n+1}(\alpha)}{J_n(\alpha)} + \beta \frac{I_{n+1}(\beta)}{I_n(\beta)} = 0 \quad (5)$$

the solutions of which give the natural frequencies of the plate:

$$\omega_n = \frac{\alpha(\phi)\beta(\phi)}{a^2} \sqrt{\frac{D}{\rho h}}. \quad (6)$$

Note that the solutions of equation (5), α and β , are functions of the tension, T , in the plate, defined by:

$$\phi = \frac{a^2 T}{14.68 D}. \quad (7)$$

Equation (7) has been defined such that $\phi = -1$ when T equals the buckling load of the plate.

Finite element analysis using the ANSYS package was performed to confirm the analytical model results. For this sensor, the two $n=2$ modes were chosen as the operational modes of the sensor, of which one is shown in figure 1.

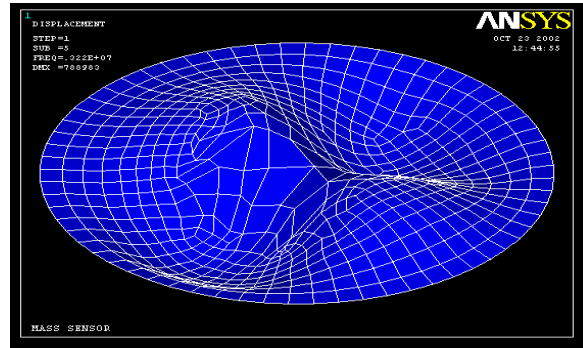


Figure 1: The resonant frequencies of the sensor were determined using an analytical model and finite element analysis.

Due to the cyclic symmetry of the structure, both the modes occur at the same frequency. However by selectively adding mass to specific areas (namely the anti-nodal positions corresponding to one mode and the nodal positions corresponding to the other mode) of the sensor, the frequency difference between the modes will become non-zero. The split $\Delta\omega$ in the natural frequencies due to the addition of mass Δm is given by:

$$\frac{\Delta\omega}{\omega} = \frac{1}{2} \frac{\Delta m}{m} + \frac{1}{2} \frac{\Delta k}{k}. \quad (8)$$

where m and k are the generalized mass and stiffness of the mode. Note that a change in stiffness Δk also contributes to this effect.

3 MANUFACTURE

An operational frequency of 5 MHz was chosen as this is well within the testing facilities available. To achieve this frequency with a $0.9 \mu\text{m}$ processing constraint on the sensor thickness a disc radius of around $50 \mu\text{m}$ was required. Stresses in the membrane layer were not expected however any present, because of the characteristics of the fabrication process, would increase the resonant frequency.

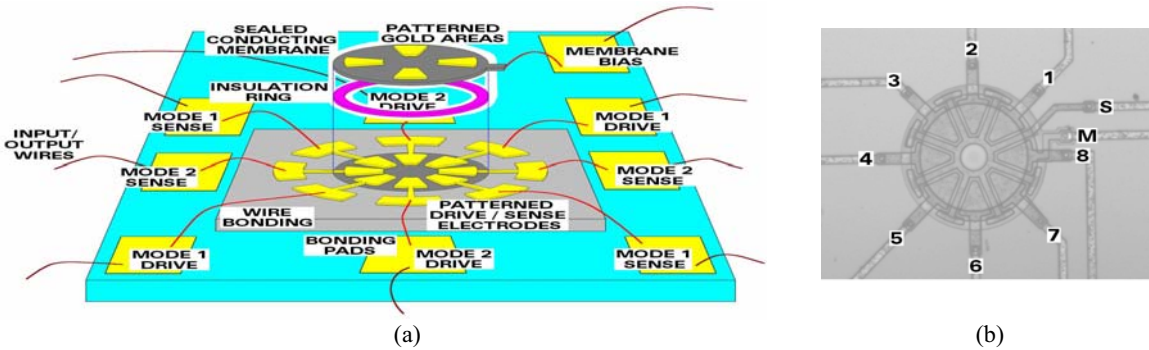


Figure 2: A schematic of the sensor (a) and the actual device (b), in this case with a diameter of $100 \mu\text{m}$. Drive / sense electrodes are numbered '1' to '8', shielding ring connection 'S' and membrane connection 'M'.

A schematic diagram of the sensor is shown in figure 2a. A polysilicon membrane forms a sealed cavity over the drive / sense electrodes and gold is patterned onto the surface of the sensor at the specific binding sites.

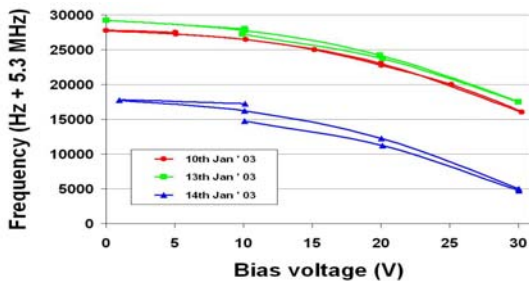
The sensor, shown in figure 2b, was manufactured by a polysilicon deposition process by NMRC (National Microelectronics Research Centre, Ireland). The sensor was manufactured using 8 variations in diameter. Each of these had an optional shielding ring and shorting of opposite electrodes, giving a total of 32 design variations.

The process flow is as follows. A 450 nm polysilicon electrode layer was deposited onto a 1.25 μm field oxide and covered with a 300 nm protective nitride layer. Two sacrificial oxide layers were then deposited, of total thickness 600 nm, followed by the 0.9 μm thick polysilicon membrane layer. After a timed HF etch to remove the sacrificial oxide, an additional 150 nm polysilicon layer was deposited to seal the membrane cavity. A final 500 nm nitride passivation layer completed the process. Note that for mechanical characterization of the sensor, the final pattern gold areas for immobilization was not processed.

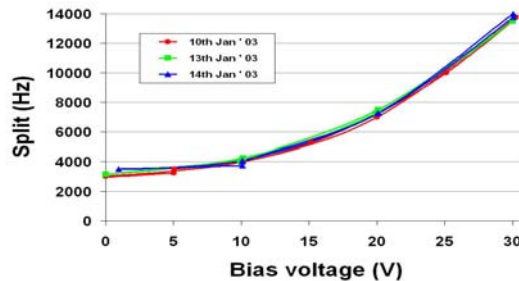
4 TESTING

The sensor was mechanically characterized using an optical workstation [6]. Both static (see figure 3) and dynamic (figure 4) tests were performed to ensure the cyclic symmetry of the device.

At this early stage of development, biological attachment protocols were not in place and to simulate the addition of mass onto the sensor, a d.c. voltage was applied across an electrode and the membrane. As shown by equation (8) this produced a frequency split between the two modes similar to the addition of mass. The measured frequency of one of the modes (taken over several days) for a range of applied voltages is given in figure 5(a). As with current sensor technology, the absolute value of the resonant frequency did drift over time. However the split between these modes (which is the operating principle of this sensor) remained constant for a given applied voltage, see figure 5(b). This initial testing clearly shows the virtue of using two degenerate vibrational modes to remove the effect of common mode noise sources, such as temperature.



(a)



(b)

Figure 5: With this sensor, as in any device, drifts occur in the absolute value of the resonant frequency due to temperature variations (a) however the frequency split (which is this sensor's operational principle) remains consistent during testing (b).

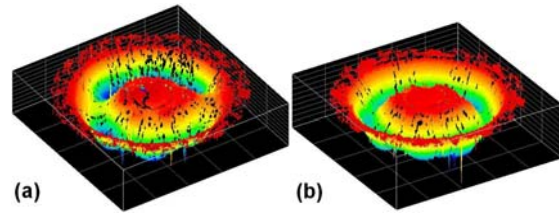


Figure (3): The deflection of the sensors under an applied voltage is used to confirm if cyclic symmetry has been achieved during manufacture: sensor (a) no, sensor (b) yes.

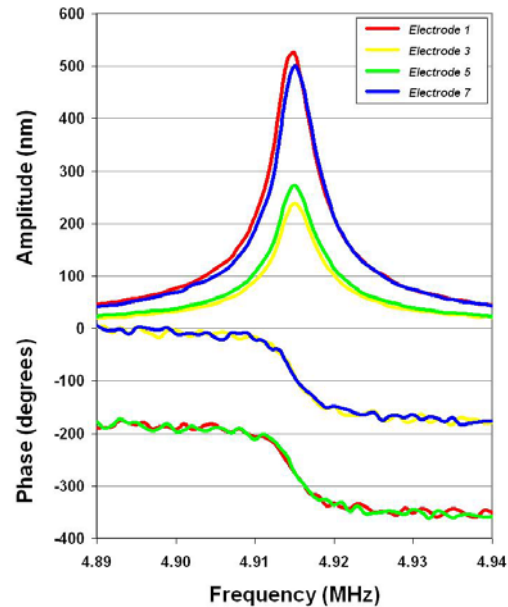


Figure (4): Vibrometer measurements are used to determine frequency and mode shape of the vibrating sensor. The phase information shows this to be the $n=2$ mode. However the amplitude data shows a slightly asymmetric vibration which is responsible for the initial frequency split between the modes prior to the addition of mass.

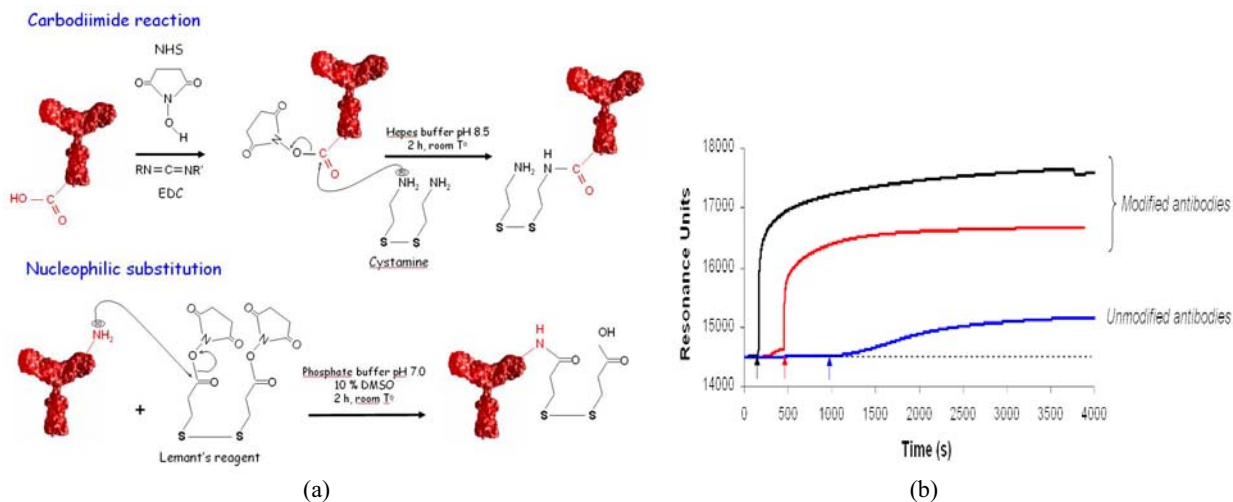


Figure 6: (a) Chemical modification of antibodies by the introduction of disulfide groups. (b) Surface plasmon resonance measurements indicate successful absorption of these modified antibodies onto a gold surface.

5 BIOLOGICAL PROTOCOLS

A study of the immobilization protocols has commenced. The introduction of disulfide groups onto the antibody structure, see figure 6(a), allows for a very strong adsorption process onto the gold surface. This feature has been characterized using surface plasmon resonance, the results of which are shown in figure 6(b). Note that the presence of these disulfide groups has increased the amount of antibody immobilized thereby increasing the sensitivity of the sensor to analyte detection.

6 CONCLUSIONS

The principle behind this mass sensor is to utilize the property of cyclic symmetry to give the device a surface mass sensitivity of the order of 0.01 ng cm^{-2} . Mechanical characterization of the sensor has been completed. Loading the sensor with an electrostatic force was used to show the measurement repeatability of the sensor over several days with these measurements being insensitive to environmental effects such as temperature variations. The biological attachment protocols are currently being investigated and the drive / sense circuitry for the sensor is under development.

7 ACKNOWLEDGEMENTS

The authors wish to acknowledge BBSRC for the research grant 13/ABY15453 and DTI for the research grant QCBC/C/002/00006.

REFERENCES

- [1] J.W. Grate, S.J. Martin and R.M. White, "Acoustic wave microsensors: Part I & II", *Analytical Chemistry* 65, 940-948 & 987-996, 1993.
- [2] S. Tombelli, M. Mascini, L. Braccini, M. Anichini and A.P.F. Turner, "Coupling of a DNA piezoelectric biosensor and polymerase chain reaction to detect apolipoprotein E polymorphisms", *Biosensors and Bioelectronics* 15, 363-370, 2000.
- [3] E. Uttenthaler, M. Schraml, J. Mandel and S. Drost, "Ultrasensitive quartz crystal microbalance sensors for detection of M13-Phages in liquids", *Biosensors and Bioelectronics* 16, 735-743, 2001.
- [4] N. Barie and M. Rapp, "Covalent bound sensing layers on surface acoustic wave (SAW) biosensors", *Biosensors and Bioelectronics* 16, 979-987, 2001.
- [5] T. Wah, "Vibration of circular plates", *Journal of the Acoustic Society of America* 34, 275-281, 1962.
- [6] J. Hedley, A. J. Harris and J. S. Burdess, "The development of a 'workstation' for optical testing and modifications of IMEMS on a wafer", *Design, Test, Integration and Packaging of MEMS/MOEMS 2001 : Proceedings of SPIE 4408*, 402-408, 2001.